J. Marine. Sci. Appl. (2009) 8: 99-104
DOI: 10.1007/s11804-009-8100-6

An application of system identification in the two-degree-freedom VIV experiments

KANG Zhuang[1*] and William C. WEBSTER[2]

1. Deepwater Engineering Research Center, Harbin Engineering University, Harbin 150001, China
2. University of California, Berkeley CA 94720-1710, USA

Abstract: Experiments on the two-degree-freedom vortex-induced vibration (VIV) of a flexibly-mounted, rigid, smooth cylinder were performed at MIT. The research reported here is an analysis of the cylinder's trajectories. System identification methods were used to derive a best Fourier representation for these motions and to parse these motions into symmetric and asymmetric behaviors. It was postulated that the asymmetric behavior was due to distortions caused by the free surface and bottom used at the test facility, and that the symmetric behavior is representative of deepwater VIV. Further application of systems identification methods was used to associate the symmetric behavior and test conditions to a traditional vortex street model. These models were analyzed for their ability to predict details of VIV trajectories.

Keywords: system identification; two-degree-freedom; vortex-induced vibration (VIV)
CLC number: O353 **Document code:** A **Article ID:** 1671-9433(2009)02-0099-06

1 Introduction

Vortex-induced vibration (VIV) of a long, flexible cylindrical structure consists of transverse oscillations in a plane normal to the axis of the structure. This phenomenon is clearly an instability of the limit-cycle type and, as a result, exhibits many typical complexities of these instabilities. These oscillations typically also vary slowly along the axis of the structure. The mechanism causing VIV is reasonably well understood as the result of periodic vortex shedding from the cylinder. However, the ability to predict the occurrence, and particularly the magnitude of VIV, is not well in hand. Sarpkaya[1] in his review of the nature of VIV pointed out that it has been known for a long time that when the vortex shedding frequency is close to the natural frequency of the cylindrical structure, vortex induced vibration will occur and the large oscillatory lift force will result in significant transverse motions of the cylinder. At the same time, the oscillatory drag force will also cause the oscillation of the cylinder in the longitudinal direction and may greatly increase the average drag of the structure. Generally, the amplitude in the longitudinal direction is smaller than in the transverse direction and the oscillation frequency is double of which in the transverse direction. VIV is particularly important in the area of ocean engineering since its consideration strongly affects the design of the large and expensive offshore structures used for oil drilling and other deep ocean tasks.

Most experimental research examined VIV using a rigid cylinder placed in uniform cross flow and restrained to have oscillations transverse to the flow. Khalak and Williamson[2] investigated VIV of an elastically mounted rigid cylinder of low mass-damping restricted to transverse oscillation. They found that there were two distinct branches in the transverse oscillation response dependent on the mass-damping parameter. Although such experiments produce VIV, there are strong indications that the longitudinal motions (in the direction of the flow) also play an important role. The existence of multiple branches in the oscillation response, however, is not limited to their simple one dimensional experiment, but can be observed in the more complex situations.

Other researchers also found some new phenomenon in the two degree of freedom VIV experiments[3-5]. Ref.[6] performed an experimental investigation of the sensitivity to small cylinder pitch rotations and in-line motions on the vortex induced lift force under the condition of transverse oscillations. The results show that an unexpected large sensitivity was found to the in-line motion that was never reported before. Ref.[7] performed an experiment on a long flexible cylinder in a shear flow. They found that the motion of the cylinder in a sheared flow could display single or multi-mode behavior depending on the power input to each of the competing modes.

Received date: 2009-02-27.
***Corresponding author Email:** kangzhuang1978@126.com

In other words, recent experimental research has shown that the VIV flow situation is complex indeed and clearly highly non-linear. Most of the research that had been performed on VIV has been performed on rather small scale models with Reynolds numbers significantly smaller than those experienced in full-scale ocean engineering situations. Our goal is two-fold. First to attempt to produce a simple theoretical model of VIV that will be useful in understanding the details of VIV, and helpful in developing a large-scale physical experiment of VIV where the Reynolds number will more closely match real ocean engineering flow situations. The research described below represents the first step in this process. The theoretical model we seek is a hybrid model based on the simple theoretical model of two-dimensional point vortices to use as a tool to help fit the experimental results, to understand better the phenomenon, and hopefully provide some predictive capability. Although such vortex models have often been attempted in the past[8], they have not been particularly successful.

What is new here is an attempt to link this model with recent excellent experimental results. For this we use some of the experimental data produced by Dahl, Hover and Triantafyllou[5] to investigate the cylinder's trajectories and to build a traditional vortex street model in an attempt to predict the details of the VIV trajectories.

2 Description of the experiments

In their paper, Dahl, Hover and Triantafyllou[5] described their experiments in details. We repeat some of this description here to set the stage for our subsequent analysis. The experiments of the two degree of freedom, vortex induced vibration of a flexibly mounted, rigid, smooth cylinder were performed at MIT. The towing tank was 2.4 m wide, 1.2 m deep and the useful test length was 22.5 m. A long, aluminum framework connected to the carriage, which is positioned along the width of the tank. A set of roller bearing was mounted to the framework that allowed motion in both vertical and horizontal directions. The test cylinder was a smooth, hollow aluminum cylinder with a diameter of 7.62 cm and a span of 200 cm. A spring bank consisted of four sets of extension springs connected to the aluminum framework and the test cylinder assembly, which allowed fine tuning of the system natural frequency in both transverse and longitudinal directions. Two linear motors were used to cancel the damping in both transverse and longitudinal directions. Fig.1 shows the whole experimental setup. The reduced velocity U_r and frequency ratio r_f are defined as follows:

$$U_r = \frac{U}{f_y D}, \qquad r_f = \frac{f_x}{f_y};$$

where U is the flow velocity, D is the diameter of the cylinder, f_y is the transverse natural frequency; and f_x is the longitudinal natural frequency.

In the experimental investigation, the data sampling frequency was 200 Hz, the reduced velocity varied from 3 to 12 in steps of 0.5 and the frequency ratio varied from 1.00 to 1.90. Details of the experiment can be found in Ref.[8].

Fig.1 General view of the experimental setup

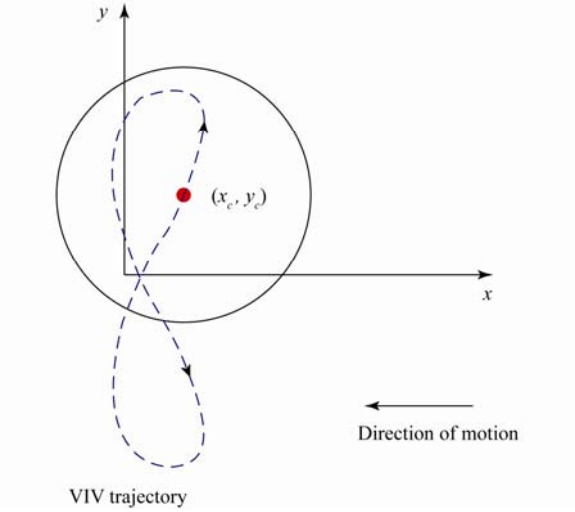

Fig.2 Coordinates used in this paper

We will use the coordinate system shown in Fig.2. The transverse coordinate is y and the coordinate along the towing tank is x (moving with the carriage and pointing away from the direction of motion). The instantaneous coordinates of the cylinder center are given by $x_c(t)$, $y_c(t)$.

3 Data processing

Ref.[8] kindly provided us with the measured trajectories of the cylinder for the frequency ratio is 1.52. In these trajectories, the reduced velocity varied from 5 to 8 at the step of 0.5. The raw data of the trajectories measured in these experiments are shown as Lissajous figures in Fig.3.

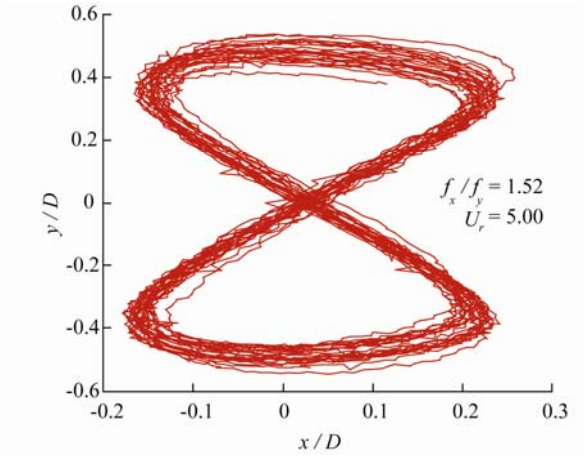

(a) $f_x / f_y = 1.52$, $U_r = 5.0$

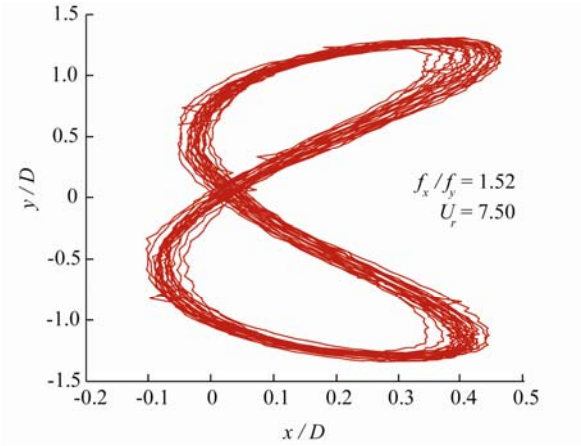

(b) $f_x / f_y = 1.52$, $U_r = 7.5$

Fig.3 Lissajous figures of the VIV measured by Dahl, Hover and Triantafyllou[8]

In these figures, the motion is normalized by the diameter of the cylinder. Although it is clear that there is considerable noise in the data and that the motions may not be quite stationary, it is of interest for our goal to find a representative trajectory for each reduced velocity for use in building our hybrid model. One should note that the vertical and horizontal scales are different in these figures (and indeed in other trajectory figures in this paper) so that the details of the motion are clear.

We first deal with the noise issue. To extract representative trajectories from the raw data, a least-squares fit was made of the data using a finite Fourier decomposition using the following assumed basis functions:

$$\begin{cases} x_c(t) = a_{0,0} + \sum_{i=1}^{5} a_{i,1}\cos(\omega t) + a_{i,2}\sin(\omega t), \\ y_c(t) = b_{0,0} + \sum_{i=1}^{5} b_{i,1}\cos(\omega t) + b_{i,2}\sin(\omega t). \end{cases} \quad (1)$$

In this least-squares fitting process the coefficients $a_{0,0}, b_{0,0}, a_{i,1}, a_{i,2}, b_{i,1}, b_{i,2}, i = 1,\cdots,5$ and the frequency ω, were all considered variables. They were determined by minimizing the squared discrepancy between $x_c(t)$, $y_c(t)$ and the corresponding raw data. Fig.4 shows two representative results of this fitting process superimposed on the original data set corresponding to a reduced velocity of 5.0 and 8.0, respectively. It is clear that the fit captures the essence of the trajectory and eliminates the noise. Within the numerical accuracy of the data and the fitting process, $a_{1,1} \approx 0$ and $a_{1,2} \approx 0$. That is, the fundamental frequency of the longitudinal motion is twice that of the transverse motion and this is consistent with the Fig.4 Lissajous figures. However, both the raw data and the fitted data are not symmetrical in the transverse direction. The characteristic Fig.4 shape of the Lissajous figure is not the same for positive y motions as for negative y motions. This non-symmetry appears to increase with increases in reduced velocity. In addition, the trajectories appear to become more incoherent as the reduced velocity increases. In particular, the trajectory of the reduced velocity of 8.0 seems particularly unsteady.

If the experimental setups were ideal, that is, if the cylinder was undergoing VIV in a tank of infinite depth and was submerged well below the free surface, then there is no physical reason why the motions should exhibit any asymmetry. It is therefore assumed that the asymmetrical part of these motions is simply an artifact of the effect of the free surface and bottom.

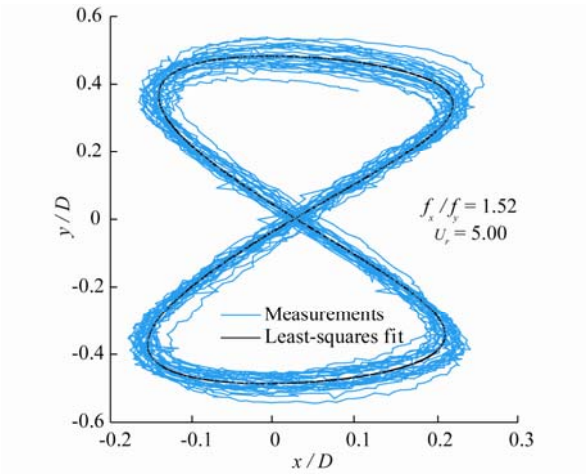

(a) $f_x / f_y = 1.52$, $U_r = 5.0$

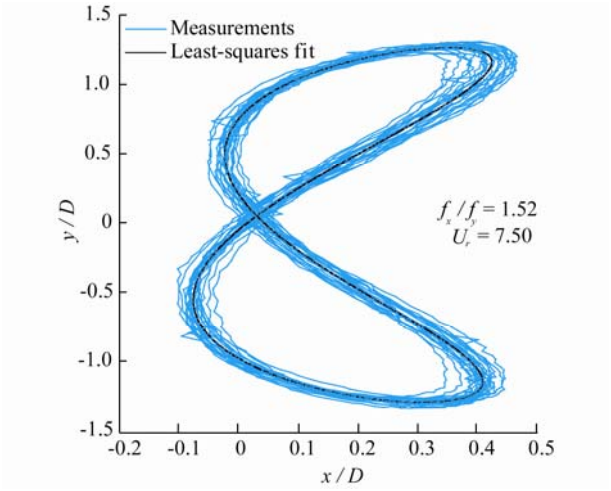

(b) $f_x / f_y = 1.52$, $U_r = 7.5$

Fig.4 Examples of the fit of the experimental data using basis functions

The next aim of the data processing was to parse the trajectory into symmetric and asymmetric parts. Before we do this, we adjust the phase of the trajectories by setting $t = \tau + \varphi$ and selecting φ such that $b_{1,1} = 0$. With this change in the t, symmetry of the Lissajous figure can be expressed as the following condition:

$$\begin{cases} x_c(t+t_0) = x_c(t+T-t_0), \\ y_c(t+t_0) = -y_c(t+T-t_0), \end{cases} \tag{2}$$

where $T = 2\pi/\omega$ is the transverse motion period.

Using this rule, the expansions in Eq.(1) can be reduced to their symmetric parts yielding

$$\begin{cases} x_c(t) = a_{0,0} + a_{2,1}\cos(\omega\tau) + a_{2,2}\sin(\omega\tau) + \\ \qquad a_{4,1}\cos(\omega\tau) + a_{4,2}\sin(\omega\tau), \\ y_c(t) = b_{1,2}\sin(\omega\tau) + b_{3,1}\cos(\omega\tau) + \\ \qquad b_{3,2}\sin(\omega\tau) + b_{5,1}\cos(\omega\tau) + b_{5,2}\sin(\omega\tau). \end{cases} \tag{3}$$

Fig.5 shows the symmetrized Lissajous figure for the reduced velocities of 5.0 and 7.5 in comparison with the original fit.

For the case of the reduced velocity of 5.0 it is seen that there is little difference between the original fit and the symmetrized fit. For the case of the reduced velocity of 7.5, the asymmetry is pronounced but the difference is still an order of magnitude smaller than the symmetric motions. An inspection of the graphs in Fig.4 also shows that as the reduced velocity increases, so does the amplitude of the transverse motion. The longitudinal motion amplitude is not monotonic, but rather increases at first and then decreases to approximately 10% of the transverse amplitude at the reduced velocity of 8.0.

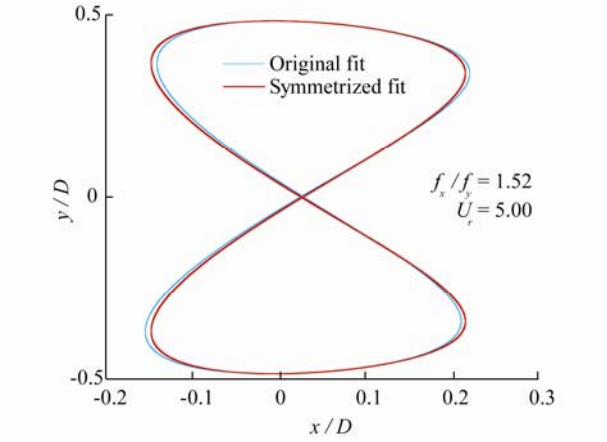

(a) $f_x / f_y = 1.52$, $U_r = 5.0$

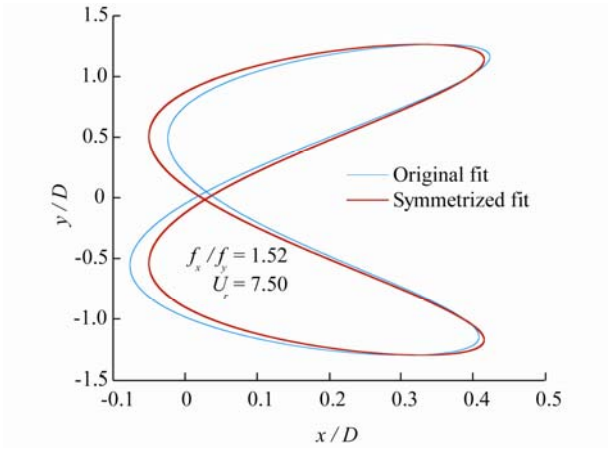

(b) $f_x / f_y = 1.52$, $U_r = 7.5$

Fig.5 Comparison of the original fit to the data and the symmetrized fit

It is the basic premise of this study that the smoothed and symmetrized trajectories produced by the above procedure represent the ideal motions of a cylinder undergoing VIV in an ideal test facility with no friction or mechanical noise and no effect resulting from the closeness of either the free surface or the bottom in the facility. The analysis below is based on this assumption.

4 Force estimation

With a smooth and symmetric VIV trajectory estimate, it is possible to analyze the hydrodynamic force history that must exist to produce this motion. The experiments of Dahl, Hover and Triantafyllou[8] used specially designed servo motors to eliminate as much as possible external damping on the cylinder. As a result, the internal mechanical forces must exactly balance the total external hydrodynamic forces, (F_x, F_y). Thus,

$$\begin{cases} F_y = m_y\,\ddot{y}_c + k_y\,y_c, \\ F_x = m_x\,\ddot{x}_c + k_x\,x_c, \end{cases} \tag{4}$$

where (m_x, m_y) are the x, y components of mass of the cylinder and attached apparatus, and (k_x, k_y) are the x, y spring constants. The components of mass are different in the x and y directions because the mass associated with the moveable parts of the test apparatus was different for these two directions.

The usual reduction of the VIV force data is purely phenomenological and does not attempt to associate the results with the actual physical processes that give rise to the forces. In this approach, the hydrodynamic forces are parsed into in-phase and out-of-phase components. The in-phase component is identified with an added-mass and the out-of-phase component with the damping. In this type of analysis one usually finds that the "added-mass" term and the "damping term" are both complicated functions of both frequency and amplitude.

A different approach is adopted here. Two-dimensional inviscid hydrodynamics predicts that the added-mass, m_a, of the cylinder equals its displaced mass. Thus, $m_a = \rho \pi r^2 l$, where ρ is the density of the water, r is the radius of the cylinder and l is the length of the cylinder. When the Reynolds number is large (as it typically is for real applications) the boundary layer around most of the cylinder is thin and it is reasonable to assume that the inviscid added-mass will continue to play an important role in the total forces on the cylinder. The remnant, the difference between the actual forces and this ideal force is then totally due to the effect of viscosity, through the development of the boundary layer around the cylinder and, most importantly, in the periodic shedding of vorticity from the cylinder. It is of interest, then, to identify this remnant so that approximate models of this phenomenon that explicitly target the effect of these shed vortices can be formulated. The computation below has this as its goal.

Eq.(4) can be re-written

$$\begin{cases} F_y = m_a\, \ddot{y}_c + [(m_y - m_a)\, \ddot{y}_c + k_x\, y_c], \\ F_x = m_a\, \ddot{x}_c + [(m_x - m_a)\, \ddot{x}_c + k_x\, x_c], \end{cases} \tag{5}$$

where the first term is what would occur in an inviscid fluid and the remaining term in brackets represents the changes that result from viscous effects.

Ref.[8] kindly provided us with the effective mechanical masses and spring constants:

$m_x =$ 23.5 kg, $k_x =$ 2850 N/m,

$m_y =$ 27.7 kg, $k_y =$ 1390 N/m,

$D =$ 7.62 cm, the cylinder diameter.

It is important to express these VIV forces as non-dimensional quantities. To do this, we divide both sides of both equations in Eq.(5) by the displacement of the cylinder, $\Delta = g\, m_a$, resulting in

$$\begin{cases} \dfrac{F_y}{\Delta} = \dfrac{D\,\ddot{\bar{y}}_c}{g} + \left[\dfrac{(m_y - m_a)}{m_a} \dfrac{D\,\ddot{\bar{y}}_c}{g} + \dfrac{(m_y + m_a)}{m_a} \dfrac{\omega_y^2\, D\, \bar{y}_c}{g} \right], \\ \dfrac{F_x}{\Delta} = \dfrac{D\,\ddot{\bar{x}}_c}{g} + \left[\dfrac{(m_x - m_a)}{m_a} \dfrac{D\,\ddot{\bar{x}}_c}{g} + \dfrac{(m_x + m_a)}{m_a} \dfrac{\omega_x^2\, D\, \bar{x}_c}{g} \right], \end{cases} \tag{6}$$

where $\bar{x}_c = x_c / D$, $\bar{y} = y_c / D$ and the natural frequencies (in water) in the x and y directions are given by

$$\omega_y = \sqrt{\frac{k_y}{m_y + m_a}}; \quad \omega_x = \sqrt{\frac{k_x}{m_x + m_a}}.$$

Inserting the known values, Eq.(6) becomes

$$\begin{cases} \dfrac{F_y}{\Delta} = 0.00777\, \ddot{\tilde{y}} + \left[0.0158\, \ddot{\tilde{y}} + 0.293\, \tilde{y} \right], \\ \dfrac{F_x}{\Delta} = 0.00777\, \ddot{\tilde{x}} + \left[0.01225\, \ddot{\tilde{x}} + 0.679\, \tilde{x} \right]. \end{cases} \tag{7}$$

The terms in the square brackets in Eq.(7) can then be used to obtain the increment in the non-dimensional transverse and longitudinal forces on these cylinders due to viscous effects.

5 Conclusions

The research reported above shows that it is possible to reduce motions data resulting from carefully controlled two-dimensional VIV experiments and to eliminate noise and asymmetries, while preserving the basic character of this phenomenon. By using the motions measured in these free oscillations, one can isolate the hydrodynamic force remnant due to viscosity and present the data in a systematic fashion.

The authors intend to use these data to help design a set of experiments of a larger scale and much higher Reynolds number (approximating that of typical offshore engineering applications). They also intend to use the techniques developed herein to analyze that data and to obtain point vortex street models of the viscous-caused forces that will hopefully aid in the prediction of this phenomenon.

References

[1] SARPKAYA T. A critical review of the intrinsic nature of vortex-induced vibrations[J]. Journal of Fluids and Structures, 2004, 19: 289-447.

[2] WILLIAMSON C H K, JAUVTIS N. A high-amplitude 2T mode of vortex-induced vibration for a light body in XY

motion[J]. European Journal of Mechanics B/Fluids, 2004, 23: 107-114.
[3] DAHL J M, HOVER F S, TRIANTAFYLLOU M S, et al. Resonant vibrations of bluff bodies cause multivortex shedding and high frequency forces[J]. Physical Review Letters, 2007, 99(14): 144503.
[4] VANDIVER J K, JONG J Y. The relationship between in-line and cross-flow vortex-induced vibration of cylinders[J]. Journal of Fluids and Structures, 1987, 1: 381-399.
[5] JAUVTIS N, WILLIAMSON C H K. Vortex-induced vibration of a cylinder with two degrees of freedom[J]. Journal of Fluids and Structures, 2003, 17: 1035–1042.
[6] de WILDE J J, HUIJSMANS R H M, TRIANTAFYLLOU M S. Experimental investigation of the sensitivity to in-line motions and magnus-like lift production on the vortex-induced vibrations[C]// Proceedings of the 13th International Offshore and Polar Engineering Conference. Honolulu, 2003: 593-598.
[7] MARCOLLOA H, HINWOOD J B. On shear flow single mode lock-in with both cross-flow and in-line lock-in mechanisms[J]. Journal of Fluids and Structures, 2006, 22: 197-211.
[8] DAHL J M, HOVER F S, TRIANTAFYLLOU M S. Two-degree-of-freedom vortex-induced vibrations using a force assisted apparatus[J]. Journal of Fluids and Structures, 2006, 22: 807–818.

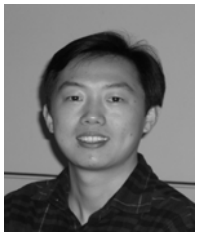

KANG Zhuang was born in 1978. He is a assosciate professor at Harbin Engineering University. His current interests is riser hydrodynamics.

William C. WEBSTER is a professor at University of California, Berkeley. His research includes investigations into nonlinear coupled motions of offshore structures, operations research, shallow water fluid mechanics, steep water waves and wave energy. He has studied the optimization, hydroelastic response, and feasibility of large-scale floating runways.

系统识别法在双自由度涡激振动试验研究中应用

康　庄[1]，William C. WEBSTER[2]

（1. 哈尔滨工程大学 深海工程技术研究中心，黑龙江 哈尔滨 150001；
2. 美国加利福尼亚大学伯克利分校，加利福尼亚 伯克利 CA 94720-1710）

摘　要：采用系统识别的方法对双自由度圆柱体的涡激振动特性进行了分析研究. 试验是在美国麻省理工大学开展，在得到的圆柱体涡激振动轨迹中，由于受到试验条件的影响，如自由液面和水池池底，得到的轨迹并非对称的“8 字形”. 因此首先对原始试验结果进行了分解，得到其傅里叶级数展开形式，然后采用了系统识别的方法对其进行分解，分别得到对称和非对称的试验结果，并认为对称的结果为理想或深海条件下圆柱体的涡激振动轨迹，而在自由液面和水池池底等其他因数的干扰下，产生了非对称的试验结果.

关键词：系统识别法；双自由度；涡激振动